Tunable Two-Photon Quantum Interference of Structured Light

Vincenzo D'Ambrosio,[1,2,*] Gonzalo Carvacho,[3] Iris Agresti,[3] Lorenzo Marrucci,[2] and Fabio Sciarrino[3,†]
[1]*ICFO—Institut de Ciencies Fotoniques, The Barcelona Institute of Science and Technology, E-08860 Castelldefels, Barcelona, Spain*
[2]*Dipartimento di Fisica, Università di Napoli Federico II, Complesso Universitario di Monte S. Angelo, 80126 Napoli, Italy*
[3]*Dipartimento di Fisica, Sapienza Università di Roma, I-00185 Roma, Italy*

(Received 7 August 2018; revised manuscript received 22 October 2018; published 4 January 2019)

Structured photons are nowadays an important resource in classical and quantum optics due to the richness of properties they show under propagation, focusing, and in their interaction with matter. Vectorial modes of light in particular, a class of modes where the polarization varies across the beam profile, have already been used in several areas ranging from microscopy to quantum information. One of the key ingredients needed to exploit the full potential of complex light in the quantum domain is the control of quantum interference, a crucial resource in fields like quantum communication, sensing, and metrology. Here we report a tunable Hong-Ou-Mandel interference between vectorial modes of light. We demonstrate how a properly designed spin-orbit device can be used to control quantum interference between vectorial modes of light by simply adjusting the device parameters and no need of interferometric setups. We believe our result can find applications in fundamental research and quantum technologies based on structured light by providing a new tool to control quantum interference in a compact, efficient, and robust way.

DOI: 10.1103/PhysRevLett.122.013601

During the last century quantum mechanics has described how even a simple object like a semitransparent surface can reveal unexpected phenomena like the Hong-Ou-Mandel (HOM) effect [1]. In this case, indeed, light exhibits a behavior that cannot be predicted by classical theory and can only be explained by considering a purely quantum effect called particle-particle interference [2]. Today bosonic coalescence is a key ingredient in photonics as it is exploited in many essential tasks: from the characterization of single photon sources to the measurement of the coherence time of photons and their degree of distinguishability. Moreover, it lies at the core of the generation of NOON states [3], a key tool in quantum metrology [4], of entanglement swapping and teleportation [5], of quantum fingerprinting [6], and quantum cloning [7–11]. Finally, quantum interference between two or more photons is nowadays a central resource in quantum computation [12–19] and quantum optics in general [20].

In the original HOM experiment two photons enter a symmetric beam splitter from two different input ports, and, if they are temporally matched, they both leave the device from the same output port (photon bunching effect) [1]. However particle-particle interference is not restricted to beam splitters and can be in general observed every time two (or more) particles are mixed in such a way that is impossible to discriminate their contribution to the final state [21–23]. Since the time delay is just one possible tunable degree of freedom for quantum interference, other control parameters could be adopted, for instance, spectral shape, path superposition, spatial modes, and polarization.

Polarization in particular is usually considered to be uniform across the beam profile; however it is possible to build vectorial beams where the polarization state varies along the transverse plane according to specific geometries. The most commonly exploited vectorial beams are those corresponding to radial and azimuthal polarization. Such states, which belong to a particular class of vector beams called vector vortex beams (VVBs) [24], show peculiar features under strong focusing [25] and symmetry properties useful for quantum communication and information [26–29]. More in general the polarization pattern can exhibit a complex structure across the beam profile with interesting applications in a plethora of fields ranging from optical trapping to metrology, nanophotonics, microscopy, and quantum information, both in classical and quantum regimes [30–36]. Despite the large development of VVB applications in the quantum domain, fully controlled quantum interference between photons in complex modes has never been observed up to now. The demonstration of a cornerstone of quantum mechanics such as the HOM effect with structured light is important both from a fundamental point of view [37] and for applications, as it could be directly implemented in quantum technologies based on structured light like the rotation invariant quantum communication protocol [26]. Here we fill this gap by reporting an experiment in which quantum interference between two photons in two different vectorial modes is observed and controlled by adjusting the parameters of a spin-orbit coupler device. By tuning two parameters of a q-plate we modify the amount of quantum interference between the two structured photons and also control the quantum phase

in the output state. Therefore, by demonstrating the possibility of tunable photon-photon interference between vectorial modes of light, our results provide a new tool for quantum experiments with structured light that allows controlling quantum interference in a compact, stable, and efficient way.

Q-plate action in the VVB space.—A convenient way to represent VVBs is through ket states $|\pi, \ell\rangle$, where π refers to the polarization state and ℓ represents a photon carrying $\ell\hbar$ quanta of orbital angular momentum [38]. Let us consider a Hilbert space spanned by states $\{|R, +m\rangle, |L, -m\rangle\}$, where $R(L)$ stands for the circular right (left) polarization state. These states correspond to light modes with a uniform circular polarization profile in an orbital angular momentum eigenstate. By considering balanced superpositions of the basis states we obtain linear polarized light modes with the polarization direction varying across the transverse profile of the beam:

$$|\hat{v}_m(\phi)\rangle = \frac{1}{\sqrt{2}}(|R, +m\rangle + e^{i\phi}|L, -m\rangle). \tag{1}$$

For each order m the VVB space can be also represented geometrically via an hybrid Poincaré sphere [39,40] where the basis states, corresponding to circular polarizations, coincide with the poles while all the linear polarized states $|\hat{v}_m(\phi)\rangle$ lie on the equator. We can define the states $\{|\hat{r}_m\rangle, |\hat{\theta}_m\rangle, |\hat{a}_m\rangle, |\hat{d}_m\rangle\}$ as $|\hat{v}_m(\phi)\rangle$ with $\phi = \{0, \pi, \pi/2, -\pi/2\}$, respectively. Following this notation, $|\hat{r}_1\rangle$ corresponds to radial polarization state and $|\hat{\theta}_1\rangle$ to the azimuthal one.

A compact way to generate and measure VVBs is through a q-plate (QP) [41], an inhomogeneous liquid crystal slab, where the orientation α of the molecular director follows the geometry $\alpha = \alpha_0 + q\varphi$, where φ is the azimuthal angle defined in the slab plane, q is the topological charge of the device, and α_0 is an offset angle. The q-plate introduces a birefringent phase shift δ that can be controlled via an externally applied voltage [42]. When $\delta = \pi$ and $q = m/2$ the q-plate acts as an interface between the polarization space and the VVB space of order m allowing one to generate and measure vector beams by simply acting in the polarization space [38,43]. Interestingly, a q-plate with topological charge $q = m$ allows one to operate transformations within the VVB space of order m [44]. The transformation matrix of this QP in the basis $\{|R, +m\rangle, |L, -m\rangle\}$ reads indeed,

$$QP[\delta, \alpha_0] = \begin{bmatrix} \cos(\delta/2) & ie^{i2\alpha_0}\sin(\delta/2) \\ ie^{-i2\alpha_0}\sin(\delta/2) & \cos(\delta/2) \end{bmatrix}. \tag{2}$$

Such transformation explicitly depends only on the retardation δ and the offset angle α_0 since the effect of the topological charge q is implicit in the mode flipping. Transformations (2) can be represented by orbits on the hybrid Poincaré sphere and can be controlled by tuning the device parameters δ and α_0 [see Figs. 1(a), 1(c)].

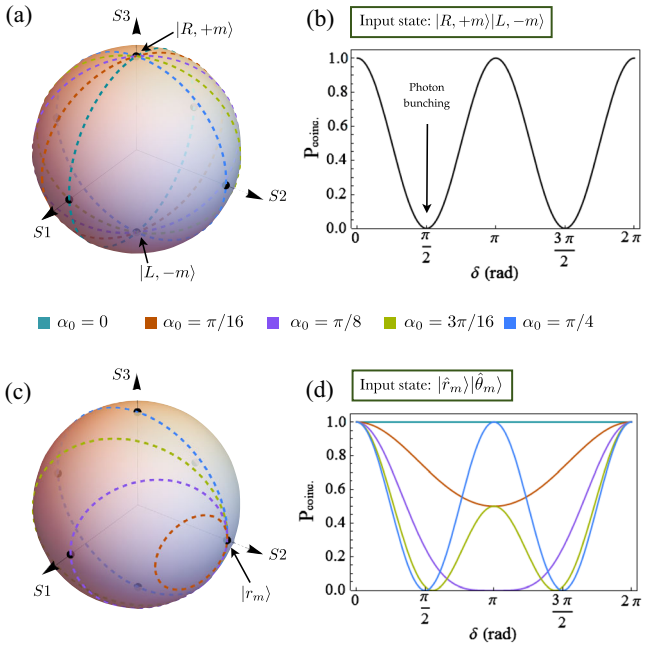

FIG. 1. Two-photon interference in a tunable q-plate: The transformation induced by a q-plate with $q = m$ on a mth order VVB can be represented by an orbit on the corresponding hybrid Poincaré sphere. Different values of α_0 correspond to different orientations of the orbits [represented by dashed circles in panels (a) and (c), one color for each α_0, and whose rotation axes lie in the S1S2 plane] while each orbit is explored by changing the retardation δ of the device. (a) When the input photon states lie on the poles the q-plate transformation orbit is a full circle for any α_0 value. (b) Two photon coincidence probability for the corresponding orbits can be tuned by changing the q-plate phase δ. Such probability does not depend on the offset angle α_0. (c) Different orbits for different angles α_0 for a state lying on the equator (in this case $|\hat{r}_m\rangle$). Each angle corresponds to a different dependence of the coincidence probability (d) with respect to the phase δ introduced by the q-plate.

When $\alpha_0 = 0$, the transformation (2) is formally equivalent to a beam splitter matrix with a tunable reflectivity that depends on δ. In particular, for $\delta = \pi/2$ the q-plate behaves as a symmetric beam splitter. The key difference with respect to a standard beam splitter is that the q-plate does not act on the direction of propagation of light but on two copropagating structured photons in different vectorial modes. Moreover, it provides an additional degree of freedom for the transformation, given by α_0.

By defining the vacuum state $|0\rangle$ and the creation operators $(a^\dagger_{1m}, a^\dagger_{2m})$ as $a^\dagger_{1m}|0\rangle = |R, +m\rangle$ and $a^\dagger_{2m}|0\rangle = |L, -m\rangle$, the transformation operated by the q-plate (2) on a two photons input state reads

$$a^\dagger_{1m}a^\dagger_{2m} \to a^\dagger_{1m}a^\dagger_{2m}\cos(\delta) + \frac{i}{2}[e^{2i\alpha_0}(a^\dagger_{1m})^2 + e^{-i2\alpha_0}(a^\dagger_{2m})^2]\sin(\delta). \tag{3}$$

For $\delta = \pi/2$ (and any value of α_0) we observe total photon bunching as the number of coincidences on the two different modes is null [Fig. 1(b)]. Moreover, the final state is a NOON state with $N = 2$ with a phase that depends on α_0 and can then be tuned by simply rotating the q-plate [44] (the only exception is the case $q = 1$, where the angle α_0 needs to be set during the manufacturing process).

When considering a generic pair of VVB states both parameters δ and α_0 have an effect on the coincidence counts. Without losing generality, we can consider the action of the q-plate on the creation operators $(a^\dagger_{r_m}, a^\dagger_{\theta_m})$ corresponding to the states $|\hat{r}_m\rangle$ and $|\hat{\theta}_m\rangle$.

The two photon state $a^\dagger_{r_m} a^\dagger_{\theta_m}|0\rangle$ is transformed in this case as follows:

$$\begin{aligned} a^\dagger_{r_m} a^\dagger_{\theta_m} \rightarrow & \\ -\sin(2\alpha_0)\sin\left(\frac{\delta}{2}\right)\left(\cos\left(\frac{\delta}{2}\right) + i\cos(2\alpha_0)\sin\left(\frac{\delta}{2}\right)\right)(a^\dagger_{r_m})^2 & \\ +\sin(2\alpha_0)\sin\left(\frac{\delta}{2}\right)\left(\cos\left(\frac{\delta}{2}\right) - i\cos(2\alpha_0)\sin\left(\frac{\delta}{2}\right)\right)(a^\dagger_{\theta_m})^2 & \\ +[\cos^2(2\alpha_0) + \cos(\delta)\sin^2(2\alpha 0)]a^\dagger_{r_m} a^\dagger_{\theta_m}. & \end{aligned} \tag{4}$$

For $\alpha_0 = 0$ the first two terms vanish and there is no quantum interference. In this case indeed $a^\dagger_{r_m}$ and $a^\dagger_{\theta_m}$ are eigenstates of the q-plate transformation; as a consequence these two states are never mixed by varying δ and they are always completely distinguishable. However, when $\alpha_0 \neq 0$ the coincidence probability depends on the phase (δ) introduced by the q-plate. Quantum interference can be controlled by tuning q-plate parameters as shown in Fig. 1(d), where the probability of measuring photon coincidences due to the $a^\dagger_{r_m} a^\dagger_{\theta_m}$ contribution are plotted as a function of the phase δ of the q-plate for different values of α_0. In the particular case of $\alpha_0 = \pi/4$ such probability is $P_{r\theta} = \cos^2(\delta)$ exactly as for the case of circular polarizations. When total photon bunching occurs, the two initially independent photons, that were in two orthogonal complex polarization modes, are forced to exit the device in the same vector vortex mode.

Although the calculation has been carried out for the states $|\hat{r}_m\rangle$ and $|\hat{\theta}_m\rangle$ the q-plate effect can be easily derived for any linear combination of $a^\dagger_{1m}$ and $a^\dagger_{2m}$. As a further example we can consider the states $|\hat{a}_m\rangle = a^\dagger_{\hat{a}_m}|0\rangle$ and $|\hat{d}_m\rangle = a^\dagger_{\hat{d}_m}|0\rangle$ that can be obtained by locally rotating the polarization direction by $\pi/4$ in $|\hat{r}_m\rangle$ and $|\hat{\theta}_m\rangle$, respectively, and, together with the other two bases here considered, form a complete set of mutually unbiased bases useful in quantum cryptography applications. Because of the geometry of these states, the only difference with respect to the previous case is that the effect of α_0 orientation is shifted by $\pi/4$ on the α_0 axis.

Observation of VVB bosonic coalescence.—To confirm the predictions of the previous section we generate a photon pair in first order VVBs and control quantum interference by tuning the parameters of a q-plate with $q = 1$. More in detail, a photon pair produced by exploiting spontaneous parametric down-conversion is sent through the experimental apparatus depicted in Fig. 2. First, the two photons go through a delay line that controls their temporal mismatch Δt. Once the photons are temporally synchronized, their polarization is rotated, so that both photons end up in the same output of a fiber polarizing beam splitter (PBS) in the state $|H,0\rangle|V,0\rangle$ where $H(V)$ stands for the linear horizontal (vertical) polarization state. In the generation stage the vector modes are created by controlling the two photon polarization states via birefringent wave plates and then by sending them through a q-plate with topological charge $q = \frac{1}{2}$ (QP1) [38]. Accordingly, vector vortex modes of order $m = 1$ are generated. For the sake of notation simplicity we will omit the subscript m from creation operators and ket states when referring to first order modes $m = 1$. We generated three different inputs: $a^\dagger_1 a^\dagger_2|0\rangle$, $a^\dagger_r a^\dagger_\theta|0\rangle$, and $a^\dagger_a a^\dagger_d|0\rangle$. After the generation, the vector vortex modes are sent through a second q-plate (QP2) with topological charge $q = 1$ to perform the transformations described by Eq. (2). Here, quantum interference takes place and can be tuned by acting on the two parameters δ and α_0 of the device. Since the $q = 1$ geometry is the only one for which α_0 cannot be tuned by simply rotating the device, we performed the experiment with two different q-plates with $\alpha_0 = \pi/4$ and $\alpha_0 = 0$, respectively. These two q-plates had been previously characterized in order to completely map the external applied voltage into the phase shift δ [42]. In the detection stage of the experiment, the two photons are sent through a third q-plate with topological charge $q = \frac{1}{2}$ (QP3) and a polarization analysis setup in order to measure photon coincidences in an arbitrary basis of the VVB space [38].

The experimental results are reported in Fig. 3 where the number of coincidences is plotted as a function of the phase shift δ introduced by QP2 when the photons are temporally synchronized $\Delta t = 0$. The three columns a, b, and c correspond to three different two-photon input states and each row to a different value of α_0. The geometry of the two q-plates are reported as insets in the plots $\alpha_0 = 0$ (top, green box) and $\alpha_0 = (\pi/4)$ (bottom, purple box). When the input state is $a^\dagger_1 a^\dagger_2|0\rangle$ [Fig. 3(a)], quantum interference depends only on the q-plate parameter δ as predicted in Fig. 1(b), showing no dependence on α_0. The coincidence counts in the basis $\{|R,+1\rangle, |L,-1\rangle\}$ are reported in Fig. 3(a) together with the best fit curve according to Eq. (3). When the input photons are in radial and azimuthal states $a^\dagger_r a^\dagger_\theta|0\rangle$ [Fig. 3(c)] the coincidence probability in the $\{|\hat{r}\rangle, |\hat{\theta}\rangle\}$ basis is constant for $\alpha_0 = 0$ but quantum interference occurs for $\alpha_0 = \pi/4$ as predicted by the Eq. (4) on

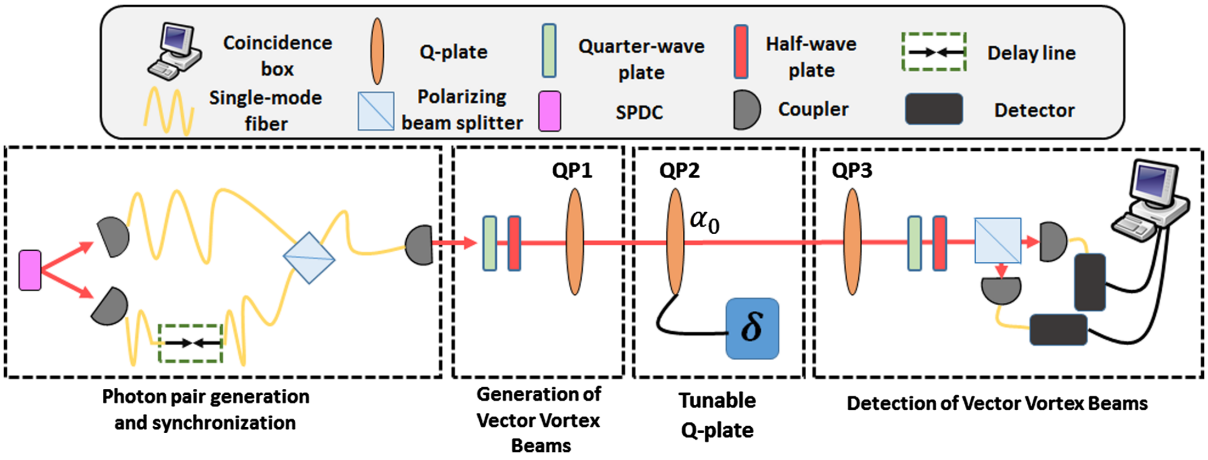

FIG. 2. Experimental apparatus. Photon pairs with orthogonal polarization are generated via the spontaneous parametric down conversion (SPDC) process, synchronized within their coherence time via a delay line and finally coupled into a fiber-based polarizing beam splitter. At the exit port of the fiber PBS, the two photons are spatially and temporally matched. In the generation stage the photons are then converted into vector vortex states by employing the q-plate QP1 with topological charge $q = 1/2$. Different polarization states (controlled with birefringent wave plates) correspond to the generation of different states in the VVB space. In the following stage the two photons pass through a second q-plate QP2 with topological charge $q = 1$ where tunable quantum interference between vectorial modes takes place. This effect is tuned by changing the parameter δ of the q-plate via an externally controlled voltage, and the offset angle α_0 (in this experiment $\alpha_0 = 0$ and $\alpha_0 = \pi/4$). In the detection stage another q-plate QP3 with topological charge $q = 1/2$ converts back the vector vortex modes into uniform polarization states, which are measured with birefringent wave plates and a bulk polarizing beam splitter. The photons are then coupled into single-mode fibers and collected by single-photon detectors connected to a coincidence box.

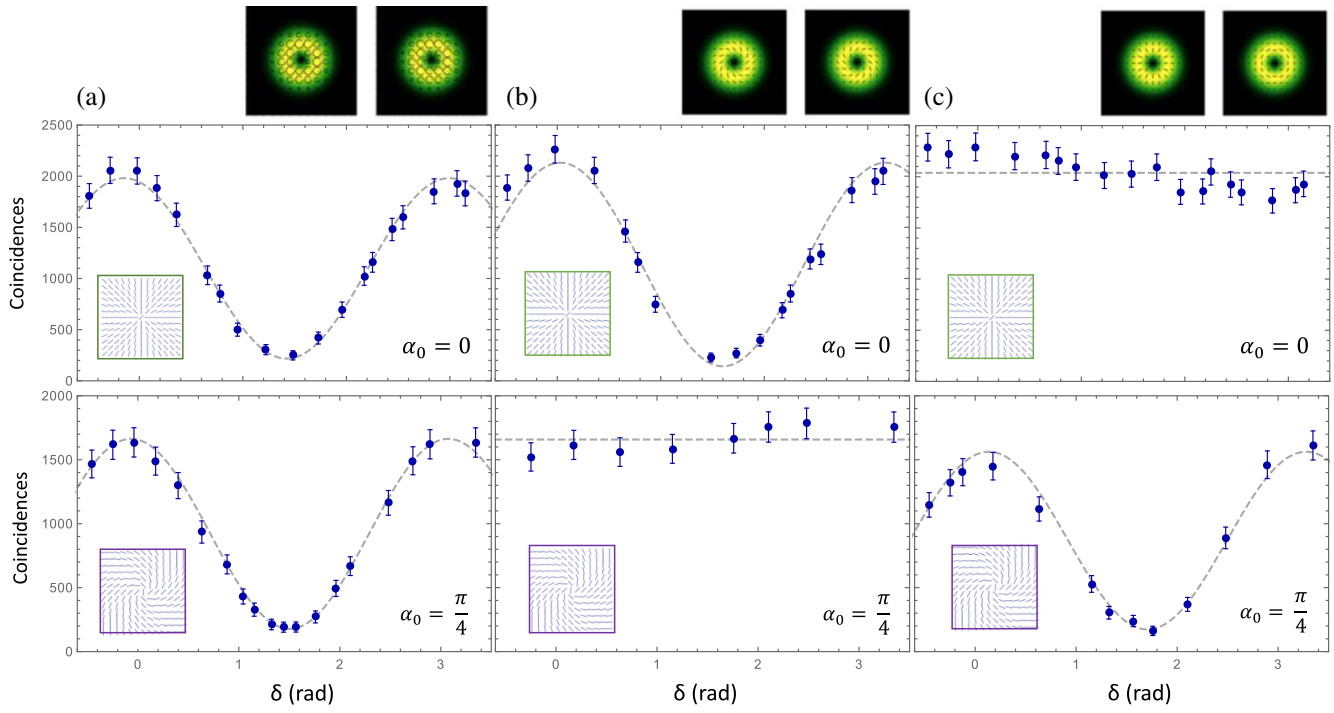

FIG. 3. Experimental tuning of photon bunching through the action of a q-plate. The six plots show the number of recorded coincidences after two-photon quantum interference takes place in QP2, as a function of the phase shift δ introduced by the device. In each panel, the colored-framed box shows the q-plate optic axis orientation. The intensity and polarization distribution in the transverse plane for the modes of the two photons is represented in two black boxes in the upper right corner of each column. All the error bars are obtained by considering a Poissonian photon statistic. (a) Input state $a_1^\dagger a_2^\dagger|0\rangle$, with $\alpha_0 = 0$ (top row, green box) and $\alpha_0 = (\pi/4)$ (bottom row, purple box); (b) input state $a_a^\dagger a_d^\dagger|0\rangle$, with $\alpha_0 = 0$ (top row, green box) and $\alpha_0 = (\pi/4)$ (bottom row, purple box); (c) input state $a_r^\dagger a_\theta^\dagger|0\rangle$, with $\alpha_0 = 0$ (top row, green box) and $\alpha_0 = (\pi/4)$ (bottom row, purple box).

which the best fit curves are based. Finally in Fig. 3(b) the coincidence probabilities for $a_a^\dagger a_d^\dagger|0\rangle$ measured in the $\{|\hat{a}\rangle, |\hat{d}\rangle\}$ basis are shown. Slight deviations from the theoretical predictions are due to experimental imperfections such as nonunitary conversion efficiency of the q-plates involved in the experiment. As predicted the behavior is similar to the radial and azimuthal case but the α_0 dependence is shifted by $\pi/4$. As a further test we measured photon coincidences as a function of the temporal delay Δt between the two photons for fixed values of δ. As expected, we observed the typical Hong-Ou-Mandel dip only when quantum interference was enabled by the q-plate action (more details in the Supplemental Material [45]).

The variety of properties that structured photons show in their propagation and interaction with matter make them an interesting resource for classical and quantum optics [34]. In the quantum domain, in particular, the large potential of structured light for quantum information applications makes it particularly relevant to develop methods to control spatial modes in the quantum regime [46]. An important step in this direction is the control over two-photon quantum interference between structured modes of light as the one reported here. Our experiment shows how a properly designed q-plate can be used to control quantum interference between vectorial modes of light by simply adjusting the device parameters. Being based on a single, thin device, our technique is intrinsically compact and stable compared to interferometric setups and can be a useful resource for quantum information processing in complex networks. An immediate application in quantum optics experiments with structured light can be the tuning of distinguishability between copropagating photons or the controlled generation of NOON states of vector beams for quantum metrology applications [33]. In quantum information our result enables the use of structured photons as carriers of information within all the protocols based on bosonic coalescence like teleportation, cloning, and entanglement swapping. As the combination of spatial modes of light with guided and integrated optics is an active research field [47,48] our work can find applications also in fiber-based and chip-based quantum information. Moreover, our result can be exploited in the automated search of new quantum experiments with structured light [49]. An additional, interesting further step can be the extension of the principle demonstrated here to multiphoton scenarios [50]. To conclude, we believe this work provides a new tool for the wide and stimulating area of fundamental research and quantum technologies based on structured light.

This work was supported by the European Union Horizon 2020 program, within the European Research Council (ERC) Grant No. 694683, PHOSPhOR. V. D. acknowledges financial support from the Spanish Ministry of Economy and Competitiveness, through the "Severo Ochoa" Programme for Centres of Excellence in R&D (SEV-2015-0522), Fundació Privada Cellex, CERCA Programme/Generalitat de Catalunya and ICFONEST fellowship program. G. C. thanks the support of Becas Chile and Conicyt.

*vincenzo.dambrosio@unina.it
†fabio.sciarrino@uniroma1.it

[1] C. K. Hong, Z. Y. Ou, and L. Mandel, Measurement of Subpicosecond Time Intervals Between Two Photons by Interference, Phys. Rev. Lett. **59**, 2044 (1987).
[2] L. Mandel, Quantum effects in one-photon and two-photon interference, Rev. Mod. Phys. **71**, S274 (1999).
[3] H. Lee, P. Kok, and J. Dowling, A quantum Rosetta stone for interferometry, J. Mod. Opt. **49**, 2325 (2002).
[4] F. Flamini *et al.*, Thermally reconfigurable quantum photonic circuits at telecom wavelength by femtosecond laser micromachining, Light Sci. Appl. **4**, e354 (2015).
[5] S. Pirandola, J. Eisert, C. Weedbrook, A. Furusawa, and S. L. Braunstein, Advances in quantum teleportation, Nat. Photonics **9**, 641 (2015).
[6] R. Chrapkiewicz, M. Jachura, K. Banaszek, and W. Wasilewski, Hologram of a single photon, Nat. Photonics **10**, 576 (2016).
[7] M. Ricci, F. Sciarrino, C. Sias, and F. De Martini, Teleportation Scheme Implementing the Universal Optimal Quantum Cloning Machine and the Universal NOT Gate, Phys. Rev. Lett. **92**, 047901 (2004).
[8] W. T. M. Irvine, A. Lamas Linares, M. J. A. de Dood, and D. Bouwmeester, Optimal Quantum Cloning on a Beam Splitter, Phys. Rev. Lett. **92**, 047902 (2004).
[9] E. Nagali, L. Sansoni, F. Sciarrino, F. De Martini, L. Marrucci, B. Piccirillo, E. Karimi, and E. Santamato, Optimal quantum cloning of orbital angular momentum photon qubits through Hong-Ou-Mandel coalescence, Nat. Photonics **3**, 720 (2009).
[10] E. Nagali, D. Giovannini, L. Marrucci, S. Slussarenko, E. Santamato, and F. Sciarrino, Experimental Optimal Cloning of Four-Dimensional Quantum States of Photons, Phys. Rev. Lett. **105**, 073602 (2010).
[11] F. Bouchard, R. Fickler, R. W. Boyd, and E. Karimi, High-dimensional quantum cloning and applications to quantum hacking, Sci. Adv. **3**, e1601915 (2017).
[12] J. B. Spring *et al.*, Boson sampling on a photonic chip, Science **339**, 798 (2012).
[13] M. Tillmann, B. Dakić, R. Heilmann, S. Nolte, A. Szameit, and P. Walther, Experimental boson sampling, Nat. Photonics **7**, 540 (2013).
[14] M. A. Broome, A. Fedrizzi, S. Rahimi-Keshari, J. Dove, S. Aaronson, T. C. Ralph, and A. G. White, Photonic boson sampling in a tunable circuit, Science **339**, 794 (2013).
[15] A. Crespi, R. Osellame, R. Ramponi, D. J. Brod, E. F. Galvão, N. Spagnolo, C. Vitelli, E. Maiorino, P. Mataloni, and F. Sciarrino, Integrated multimode interferometers with arbitrary designs for photonic boson sampling, Nat. Photonics **7**, 545 (2013).
[16] J. Carolan *et al.*, On the experimental verification of quantum complexity in linear optics, Nat. Photonics **8**, 621 (2014).
[17] J. Carolan *et al.*, Universal linear optics, Science **349**, 711 (2015).

[18] M. Bentivegna *et al.*, Experimental scattershot boson sampling, Sci. Adv. **1**, e1400255 (2015).
[19] J. C. Loredo, M. A. Broome, P. Hilaire, O. Gazzano, I. Sagnes, A. Lemaitre, M. P. Almeida, P. Senellart, and A. G. White, Boson Sampling with Single-Photon Fock States from a Bright Solid-State Source, Phys. Rev. Lett. **118**, 130503 (2017).
[20] J.-W. Pan, Z.-B. Chen, C.-Y. Lu, H. Weinfurter, A. Zeilinger, and M. Żukowski, Multiphoton entanglement and interferometry, Rev. Mod. Phys. **84**, 777 (2012).
[21] N. Spagnolo, C. Vitelli, L. Aparo, P. Mataloni, F. Sciarrino, A. Crespi, R. Ramponi, and R. Osellame, Three-photon bosonic coalescence in an integrated tritter, Nat. Commun. **4**, 1606 (2013).
[22] S. Agne, T. Kauten, J. Jin, E. Meyer-Scott, J. Z. Salvail, D. R. Hamel, K. J. Resch, G. Weihs, and T. Jennewein, Observation of Genuine Three-Photon Interference, Phys. Rev. Lett. **118**, 153602 (2017).
[23] A. J. Menssen, A. E. Jones, B. J. Metcalf, M. C. Tichy, S. Barz, W. Steven Kolthammer, and I. A. Walmsley, Distinguishability and Many-Particle Interference, Phys. Rev. Lett. **118**, 153603 (2017).
[24] Q. Zhan, Cylindrical vector beams: From mathematical concepts to applications, Adv. Opt. Photonics **1**, 1 (2009).
[25] R. Dorn, S. Quabis, and G. Leuchs, Sharper Focus for a Radially Polarized Light Beam, Phys. Rev. Lett. **91**, 233901 (2003).
[26] V. D'Ambrosio, E. Nagali, S. P. Walborn, L. Aolita, S. Slussarenko, L. Marrucci, and F. Sciarrino, Complete experimental toolbox for alignment-free quantum communication, Nat. Commun. **3**, 961 (2012).
[27] G. Vallone, V. D'Ambrosio, A. Sponselli, S. Slussarenko, L. Marrucci, F. Sciarrino, and P. Villoresi, Free-Space Quantum Key Distribution by Rotation-Invariant Twisted Photons, Phys. Rev. Lett. **113**, 060503 (2014).
[28] V. Parigi, V. D'Ambrosio, C. Arnold, L. Marrucci, F. Sciarrino, and J. Laurat, Storage and retrieval of vector beams of light in a multiple-degree-of-freedom quantum memory, Nat. Commun. **6**, 7706 (2015).
[29] O. J. Farías, V. D'Ambrosio, C. Taballione, F. Bisesto, S. Slussarenko, L. Aolita, L. Marrucci, S. P. Walborn, and F. Sciarrino, Resilience of hybrid optical angular momentum qubits to turbulence, Sci. Rep. **5**, 8424 (2015).
[30] B. J. Roxworthy and K. C. J. Toussaint, Optical trapping with π-phase cylindrical vector beams, New J. Phys. **12**, 073012 (2010).
[31] M. Neugebauer, P. Banzer, T. Bauer, S. Orlov, N. Lindlein, A. Aiello, and G. Leuchs, Geometric spin Hall effect of light in tightly focused polarization-tailored light beams, Phys. Rev. A **89**, 013840 (2014).
[32] R. Fickler, R. Lapkiewicz, S. Ramelow, and A. Zeilinger, Quantum entanglement of complex photon polarization patterns in vector beams, Phys. Rev. A **89**, 060301 (2014).
[33] V. D'Ambrosio, N. Spagnolo, L. Del Re, S. Slussarenko, Y. Li, L. C. Kwek, L. Marrucci, S. P. Walborn, L. Aolita, and F. Sciarrino, Photonic polarization gears for ultra-sensitive angular measurements, Nat. Commun. **4**, 2432 (2013).
[34] H. Rubinsztein-Dunlop *et al.*, Roadmap on structured light, J. Opt. **19**, 013001 (2017).
[35] C. Maurer, A. Jesacher, S. Furhapter, S. Bernet, and M. Ritsch-Marte, Tailoring of arbitrary optical vector beams, New J. Phys. **9**, 78 (2007).
[36] A. Büse, M. L. Juan, N. Tischler, V. D'Ambrosio, F. Sciarrino, L. Marrucci, and G. Molina-Terriza, Symmetry Protection of Photonic Entanglement in the Interaction with a Single Nanoaperture, Phys. Rev. Lett. **121**, 173901 (2018).
[37] T. B. Pittman, D. V. Strekalov, A. Migdall, M. H. Rubin, A. V. Sergienko, and Y. H. Shih, Can Two-Photon Interference be Considered the Interference of Two Photons?, Phys. Rev. Lett. **77**, 1917 (1996).
[38] V. D'Ambrosio, G. Carvacho, F. Graffitti, C. Vitelli, B. Piccirillo, L. Marrucci, and F. Sciarrino, Entangled vector vortex beams, Phys. Rev. A **94**, 030304 (2016).
[39] G. Milione, H. I. Sztul, D. A. Nolan, and R. R. Alfano, Higher-Order Poincaré Sphere, Stokes Parameters, and the Angular Momentum of Light, Phys. Rev. Lett. **107**, 053601 (2011).
[40] A. Holleczek, A. Aiello, C. Gabriel, C. Marquardt, and G. Leuchs, Classical and quantum properties of cylindrically polarized states of light, Opt. Express **19**, 9714 (2011).
[41] L. Marrucci, C. Manzo, and D. Paparo, Optical Spin-to-Orbital Angular Momentum Conversion in Inhomogeneous Anisotropic Media, Phys. Rev. Lett. **96**, 163905 (2006).
[42] B. Piccirillo, V. D'Ambrosio, S. Slussarenko, L. Marrucci, and E. Santamato, Photon spin-to-orbital angular momentum conversion via an electrically tunable q-plate, Appl. Phys. Lett. **97**, 241104 (2010).
[43] F. Cardano, E. Karimi, S. Slussarenko, L. Marrucci, C. de Lisio, and E. Santamato, Polarization pattern of vector vortex beams generated by q-plates with different topological charges, Appl. Opt. **51**, C1 (2012).
[44] V. D'Ambrosio, F. Baccari, S. Slussarenko, L. Marrucci, and F. Sciarrino, Arbitrary, direct and deterministic manipulation of vector beams via electrically-tuned q-plates, Sci. Rep. **5**, 7840 (2015).
[45] See Supplemental Material at http://link.aps.org/supplemental/10.1103/PhysRevLett.122.013601 for more experimental details.
[46] M. Erhard, R. Fickler, M. Krenn, and A. Zeilinger, Twisted photons: New quantum perspectives in high dimensions, Light Sci. Appl. **7**, 17146 (2018).
[47] X. Cai, J. Wang, M. J. Strain, B. Johnson-Morris, J. Zhu, M. Sorel, J. L. O'Brien, M. G. Thompson, and S. Yu, Integrated compact optical vortex beam emitters, Science **338**, 363 (2012).
[48] N. Bozinovic, Y. Yue, Y. Ren, M. Tur, P. Kristensen, H. Huang, A. E. Willner, and S. Ramachandran, Terabit-scale orbital angular momentum mode division multiplexing in fibers, Science **340**, 1545 (2013).
[49] M. Krenn, M. Malik, R. Fickler, R. Lapkiewicz, and A. Zeilinger, Automated Search for New Quantum Experiments, Phys. Rev. Lett. **116**, 090405 (2016).
[50] M. Tillmann, S.-H. Tan, S. E. Stoeckl, B. C. Sanders, H. de Guise, R. Heilmann, S. Nolte, A. Szameit, and P. Walther, Generalized Multiphoton Quantum Interference, Phys. Rev. X **5**, 041015 (2015).